


## ORIGINAL ARTICLE

# Junction plakoglobin regulates and destabilizes HIF2 $\alpha$ to inhibit tumorigenesis of renal cell carcinoma

Ke Chen<sup>1,2,†</sup> | Jin Zeng<sup>1,2,3,†</sup>  | Yi Sun<sup>1,2</sup> | Wei Ouyang<sup>1,2</sup> | Gan Yu<sup>1,2</sup> | Hui Zhou<sup>1,2</sup> | Yangjun Zhang<sup>1,2</sup> | Weimin Yao<sup>1,2</sup> | Wei Xiao<sup>1,2</sup> | Junhui Hu<sup>2,4</sup> | Jinchun Xing<sup>5</sup> | Kefeng Xiao<sup>6</sup> | Lily Wu<sup>4</sup> | Zhiqiang Chen<sup>1,2</sup> | Zhangqun Ye<sup>1,2</sup> | Hua Xu<sup>1,2</sup>

<sup>1</sup> Department of Urology, Tongji Hospital, Tongji Medical College, Huazhong University of Science and Technology, Wuhan, Hubei 430030, P. R. China

<sup>2</sup> Hubei Institute of Urology, Wuhan, Hubei 430030, P. R. China

<sup>3</sup> Department of Urology, The First Affiliated Hospital of Nanchang University, Nanchang, Jiangxi 330000, P. R. China

<sup>4</sup> Department of Molecular and Medical Pharmacology, David Geffen School of Medicine, University of California at Los Angeles, Los Angeles, CA 90095, USA

<sup>5</sup> Department of Urology, The First Affiliated Hospital of Xiamen University, Xiamen, Fujian 361003, P. R. China

<sup>6</sup> Department of Urology, The People's Hospital of Shenzhen City, Shenzhen, Guangdong 518020, P. R. China

## Correspondence

Hua Xu, Department of Urology, Tongji Hospital, Tongji Medical College, Huazhong University of Science and Technology, Wuhan 430030, Hubei, P. R. China.  
 Email: xuhua@hust.edu.cn

<sup>†</sup>These authors contributed equally to this work.

## Abstract

**Background:** Increased hypoxia-inducible factor 2 $\alpha$  (HIF2 $\alpha$ ) activation is a common event in clear cell renal cell carcinoma (ccRCC) progression. However, the function and underlying mechanism of HIF2 $\alpha$  in ccRCC remains uninvestigated. We conducted this study to access the potential link between junction plakoglobin (JUP) and HIF2 $\alpha$  in ccRCC.

**Methods:** Affinity purification and mass spectrometry (AP-MS) screening, glutathione-s-transferase (GST) pull-down and co-immunoprecipitation (Co-IP) assays were performed to detect the interacting proteins of HIF2 $\alpha$ . Quantitative PCR (qPCR) and Western blotting were used to detect the expression of JUP in human ccRCC samples. Luciferase reporter assays, chromatin immunoprecipitation (ChIP), cycloheximide chase assays, and ubiquitination assays were conducted to explore the regulation of JUP on the activity of HIF2 $\alpha$ . Cell Counting Kit-8 (CCK-8) assays, colony formation assays, transwell assays, and xenograft

**Abbreviations:** JUP, Junction plakoglobin; HIF2 $\alpha$ , Hypoxia-inducible factor 2 alpha; EGLN1, Egl-9 family hypoxia inducible factor 1; ccRCC, Clear cell renal cell carcinoma; RCC, Renal cell carcinoma; AP-MS, Affinity purification coupled with mass spectrometry; qPCR, Quantitative PCR; RT-PCR, Real time PCR; ChIP, Chromatin immunoprecipitation; VHL, von Hippel-Lindau; PTMs, Post-translational modifications; CBP, cAMP-response element binding protein; HDACs, Histone deacetylases; HREs, Hypoxia response elements; ARNT, Aryl hydrocarbon receptor nuclear translocator; TCGA, The Cancer Genome Atlas; PAS, Per-Arnt-Sim; DM, Double mutant; Co-IP, Co-Immunoprecipitation; CCK-8, Cell Counting Kit-8; SDS-PAGE, sodium dodecyl sulfate polyacrylamide gel electrophoresis; GST, Glutathione-S-transferases; CUL2, Cullin 2; EGFP, Enhanced Green Fluorescent Protein; TCF-4, Transcription Factor 4; TBP, TATA-Box Binding Protein; IH, inhibitory; PAS, the Per-Arnt-Sim; PAC, PAS-associated C-terminal

This is an open access article under the terms of the [Creative Commons Attribution-NonCommercial-NoDerivs](https://creativecommons.org/licenses/by-nc-nd/4.0/) License, which permits use and distribution in any medium, provided the original work is properly cited, the use is non-commercial and no modifications or adaptations are made.

© 2021 The Authors. *Cancer Communications* published by John Wiley & Sons Australia, Ltd. on behalf of Sun Yat-sen University Cancer Center

tumor assays were performed to investigate the effect of JUP knockdown or overexpression on the tumorigenicity of renal cancer cells.

**Results:** We identified JUP as a novel HIF2 $\alpha$ -binding partner and revealed an important role of JUP in recruiting von Hippel-Lindau (VHL) and histone deacetylases 1/2 (HDAC1/2) to HIF2 $\alpha$  to regulate its stability and transactivation. JUP knockdown promoted and overexpression suppressed the tumorigenicity of renal cell carcinoma in vitro and in vivo. Importantly, the low expression of JUP was found in clinical ccRCC samples and correlated with enhanced hypoxia scores and poor treatment outcomes.

**Conclusion:** Taken together, these data support a role of JUP in modulating HIF2 $\alpha$  signaling during ccRCC progression and identify JUP as a potential therapeutic target.

#### KEYWORDS

renal cell carcinoma, junction plakoglobin, hypoxia-inducible factor 2 $\alpha$ , transcriptional activity, ubiquitination

## 1 | BACKGROUND

Renal cell carcinoma (RCC) is a common urologic tumor, accounting for more than 144,000 deaths each year [1], and clear cell renal cell carcinoma (ccRCC) is the most common histological type. Most ccRCC cases are due to loss of the tumor suppressor gene von Hippel-Lindau (VHL) [2]. The best-known function of VHL is as an E3 ubiquitin ligase that targets hypoxia-inducible factor 1 $\alpha$  (HIF1 $\alpha$ ) and HIF2 $\alpha$  for degradation [3]. However, HIF1 $\alpha$  inhibits the initiation and/or progression of ccRCC, whereas HIF2 $\alpha$  acts as an oncogene [4]. Extensive studies have revealed that hyperactivation of HIF2 $\alpha$  signaling is a central module of cell survival and metastasis in ccRCC [5]. Apart from VHL-mediated ubiquitination, HIF2 $\alpha$  activity is also regulated at various levels involving other post-translational modifications (PTMs) and cofactors. In hypoxic cells, cAMP-response element binding protein (CBP) catalyzes the acetylation of lysine residues of HIF2 $\alpha$ , which acts in conjunction with sirtuin 1 to promote HIF2 $\alpha$  signaling [6, 7]. Epigenetic regulators are also involved in HIF2 $\alpha$ -mediated transactivation. For example, HIFs recruit histone deacetylases (HDACs) and p300/CBP to regulate the expression of some HIF-responsive genes [8, 9]. In addition, zinc finger MYND-type containing 8 promotes the transcriptional activity of both HIF1 $\alpha$  and HIF2 $\alpha$  by recruiting bromodomain-containing protein 4 to the hypoxia response elements (HREs), which induces the release of paused RNA polymerase II [10]. Importantly, there is evidence for crosstalk between HIF2 $\alpha$  signaling and many other pathways, such as nuclear factor kappa-B (NF- $\kappa$ B) [11, 12], Notch signaling [13, 14], and

Wnt/ $\beta$ -catenin signaling [15, 16], in various cancers including ccRCC.

Due to the fundamental role of HIF2 $\alpha$  in ccRCC, structure-based drug design and rational modification has led to the development of a novel series of drugs, such as PT2385, PT2399, and PT2977, which can disrupt HIF2 $\alpha$ /aryl hydrocarbon receptor nuclear translocator (ARNT) heterodimerization and inhibit HIF2 $\alpha$  target gene expression [17–19]. Additionally, a phase I trial showed PT2385 had a favorable safety profile and was active in patients with advanced ccRCC who had previously taken a tyrosine kinase inhibitor [20]. However, many challenges still exist, such as differential sensitivity and the development of therapy resistance to HIF2 $\alpha$  antagonists [18]; the function and underlying mechanism of HIF2 $\alpha$  in tumorigenesis remains uninvestigated.

Given that HIF2 $\alpha$  is a good therapeutic target for ccRCC treatment and the regulatory factors of HIF2 $\alpha$  are still not clear, we sought to investigate the key molecules that could regulate the activity of HIF2 $\alpha$ . Therefore, we screened the interaction proteins of HIF2 $\alpha$  by affinity purification-MS (AP-MS). Our study aimed to investigate the interaction between JUP and HIF2 $\alpha$  and whether HIF2 $\alpha$  signaling is regulated by JUP during ccRCC progression.

## 2 | MATERIALS AND METHODS

### 2.1 | Human samples

ccRCC and corresponding adjacent normal tissues were obtained from 12 ccRCC patients treated in the

Department of Urology at Tongji Hospital (Wuhan, Hubei, China) between January 2013 and August 2013 after they provided written informed consent. All samples were kept in liquid nitrogen before RNA and protein extraction. A ccRCC tissue array was purchased from Shanghai Superchip (HKidCRC030PG01; Shanghai, China).

## 2.2 | Antibodies

The following antibodies were used in the experiments: mouse anti-glyceraldehyde-3-phosphate dehydrogenase (GAPDH) (G8795, 1:10,000) and anti-Flag (F3165, 1:2000) from Sigma-Aldrich (St. Louis, MO, USA); mouse anti-Myc (11667149001, 1:2000) and mouse anti-hemagglutinin (HA) antibody (11583816001, 1:2000) from Roche Applied Science (Penzberg, Germany); rabbit anti-Myc (562, 1:2000), rabbit anti-HA antibody (561, 1:2000), and anti-Strep-tag II (M211-3, 1:3000) from MBL Life Science (MBL, Nagoya, Japan); anti-HIF2 $\alpha$  (NB100-122, 1:1000) from Novus Biologicals (Centennial, CO, USA); anti-histone H3 (acetyl K27) (H3K27ac, 1:100 for ChIP) (ab4729) from Abcam (Cambridge, MA, USA); anti-HDAC1 (GTX100513) from GeneTex (Irvine, CA, USA); rabbit anti-junction plakoglobin (JUP) (#75550, 1:1000) and anti-p300 (#86377, 1:100 for ChIP) from Cell Signaling Technology (Danvers, MA, USA); mouse anti-JUP (#MA5-15905, 1:1000), goat anti-mouse IgG secondary antibody (31430, 1:20,000), and goat anti-rabbit IgG-horseradish peroxidase (HRP) secondary antibody (31460, 1:20,000) from Thermo Fisher Scientific (Waltham, MA, USA).

## 2.3 | Cell lines, cell culture, transfection, virus infection and treatments

The 786-O, OSRC-2, SN12-PM6, ACHN, and HEK293T cell lines were purchased from the Cell Bank of Shanghai Institute of Cell Biology (Chinese Academy of Medical Science, Shanghai, China). These cells were cultured in Dulbecco's Modified Eagle's Medium (DMEM, HyClone, Logan, Utah, USA) with 10% fetal bovine serum (HyClone) in the presence of 5% CO<sub>2</sub> at 37°C in a humidified incubator (Thermo Fisher Scientific). Transfection was performed using Lipofectamine™2000 (Thermo Fisher Scientific). For lentiviral infection, HEK293T cells were transfected with packaging vectors (pRSV-Rev, pMD2.G, and pCMV-VSV-G) and LacZ shRNA, JUP shRNA, HIF2 $\alpha$  shRNA plasmids, or psi-HA-JUP plasmids; the viruses were collected 60 h after transfection and used to infect 786-O or ACHN cells. Stably transduced cells were screened using puromycin (Sigma) at a final concentration of 2 mg/mL for 3 days. Cells were treated with 10  $\mu$ g/mL MG132 (S1748,

Beyotime Biotechnology, Beijing, China) for 6 h before being harvested for immunoblotting with anti-HIF2 $\alpha$  antibody or control antibodies.

## 2.4 | RT-PCR analysis

Total RNAs were extracted by TRIzol (Invitrogen, Carlsbad, CA, USA) and cDNAs were synthesized using the ReverTra Ace qPCR RT Kit (Toyobo, Osaka, Japan). Real-time PCR (qPCR) was performed following standard protocols using SYBR Green Mix (Roche). The primer sequences used are shown in Supplementary Table S1.

## 2.5 | Luciferase assay

HEK293T or 786-O cells were grown in 48-well plates to 50%-70% confluency and transfected with 6xHRE-Luc, pRL-TK, Flag-HIF2 $\alpha$ , and HA-JUP overexpressed plasmid combinations using Lipofectamine™2000 (Thermo Fisher Scientific). Approximately 36 h after transfection, cells were lysed and analyzed using the Dual-Luciferase Reporter System (Promega, Fitchburg, WI, USA).

## 2.6 | Plasmids

VHL, Myc-ubiquitin, EGFP-HIF1 $\alpha$ , TK-Rluc, and 6xHRE-Luc plasmids have been previously described [21, 22]. All the other plasmids in this study were constructed by standard molecular biology techniques. psi-StrepII, which contains Strep-tag-II, was constructed by inserting two Strep-tag sequences into the psi-Flag plasmid. PCDH-StrepII-GST-C1, containing fusion tags including Strep-tag-II and GST-tag, was constructed by subcloning Strep-tag-II and GST-tag into the XbaI and NotI sites of PCDH-CD513B-1 (System Biosciences, Palo Alto, CA, USA). The 12xHis-tag sequence was synthesized and cloned into PCDH-StrepII-GST-C1 to obtain PCDH-12xHis. Wild-type (WT) HIF2 $\alpha$  cDNA was PCR-amplified using primers HIF2 $\alpha$ -5' and HIF2 $\alpha$ -3', digested by BamHI and SalI, and ligated into pEGFP-myc-C1, psi-StrepII, PCDH-12xHis, and psi-Flag to create EGFP-myc-HIF1 $\alpha$ , StrepII-HIF2 $\alpha$ , 12xHis-HIF2 $\alpha$ , and Flag-HIF2 $\alpha$ , respectively. JUP cDNA was PCR-amplified using primers JUP-5' and JUP-3', digested by BamHI and XhoI, and ligated into psi-HA, pGEX-4T-1, and PCDH-StrepII-GST-C1 to create HA-JUP, GST-JUP (bacterial expression plasmid), and StrepII-GST-JUP (mammalian expression plasmid). Mammalian expression plasmids for human ARNT, HDAC1, HDAC2, and deletion mutants of HIF2 $\alpha$  and JUP were constructed using standard molecular biology

techniques. The PCDH-H1 short hairpin RNA (shRNA) cloning vector was constructed by enzymatically deleting the cytomegalovirus (CMV) promoter of the PCDH-CD513B-1 plasmid, and then inserting the H1 promoter of pSilencer5.1-H1 Retro plasmid (Thermo Fisher Scientific). The shRNA target sequence was synthesized and inserted into the BamHI and NotI sites of PCDH-H1. The target sequences for shRNA JUP, HIF2 $\alpha$ , or HDAC1 were as follows: sh-JUP-1#, 5'-GCTTCAGACTCAAGTACCCA-3'; sh-JUP-2#, 5'-GATCATGCGTAACTACAGTTA-3'; sh-HIF2 $\alpha$ -1#, 5'-GATGGACTTACCTGGCAGAC-3'; sh-HIF2 $\alpha$ -2#, 5'-GCTGACCAGCAGATGGACAAC-3'; and sh-HDAC1, 5'-GCAGATGCAGAGATTCAACG-3'. The primers used are shown in Supplementary Table S1.

## 2.7 | Co-immunoprecipitation (Co-IP)

To analyze protein interactions, Co-IP experiments were performed using HEK293T or 786-O cells after 48-hour transfection. Then, the cells were lysed in NETN lysis buffer (50 mmol/L Tris-HCl at pH 8.0, 0.15 M NaCl, 1 mmol/L EDTA, 0.5% NP-40) with a 1 $\times$  protease inhibitor cocktail (Roche). Specified antibody and Protein G Agarose (Roche) were incubated with the cell lysates overnight at 4°C. The resins were washed four times with wash buffer (50 mmol/L Tris-HCl at pH 8.0, 0.5 mol/L NaCl, 1 mmol/L EDTA, 0.5% NP-40). After elution by loading buffer, the bound proteins were separated by sodium dodecyl sulfate polyacrylamide gel electrophoresis (SDS-PAGE).

## 2.8 | Cycloheximide chase assays

For pulse-chase analysis, cells were aliquoted to 35 mm dishes. When achieved 80%–90% confluence, the cells were treated with cycloheximide (CHX, A10036, AdooQ BioScience, Irvine, CA, USA) at a final concentration of 100  $\mu$ mol/L. At the indicated time points after CHX treatment, the cells were harvested for immunoblotting with anti-HIF2 $\alpha$  antibody or control antibodies.

## 2.9 | Ubiquitination assays

ACHN cells transfected with 12  $\times$  HIS-HIF2 $\alpha$ , Myc-ubiquitin (Myc-UB), and HA-JUP were treated with 10  $\mu$ g/mL MG132 for 6 h before being lysed with UREA buffer (10 mmol/L Tris-HCl at pH 8.0, 100 mmol/L NaH<sub>2</sub>PO<sub>4</sub>, 8 mol/L urea, 10 mmol/L imidazole). After sonication, the lysate was centrifuged at 12,000  $\times$  g for 10 min at 4°C. Then, supernatant was incubated with Ni-NTA Superflow agarose (Thermo Fisher Scientific) for 4 h at

room temperature. The beads were washed four times with UREA buffer containing 20 mmol/L imidazole.

## 2.10 | AP-MS

Cells (~100 million) stably expressing StrepII or StrepII-HIF2 $\alpha$  were lysed in NETN lysis buffer consisting of 50 mmol/L Tris-HCl at pH 8.0, 0.15 mol/L NaCl, 1 mmol/L ethylenediaminetetraacetic acid (EDTA), 0.5% NP-40, and a 1 $\times$  protease inhibitor cocktail (Roche). Prior to complex purification, avidin (20  $\mu$ g/mL extracts, A9275; Sigma) was added to the extracts to remove biotinylated molecules that may bind nonspecifically to the Strep-Tactin XT superflow resin (2–4010; IBA Lifesciences, Gottingen, Germany). Then the superflow resin (80  $\mu$ L) was added to the extracts followed by incubation for 4 h at 4°C. Beads were washed five times with wash buffer and then eluted with NuPAGE™ LDS Sample Buffer (NP0007; Thermo Fisher Scientific). The proteins were separated by SDS-PAGE (NP0322BOX; Thermo Fisher Scientific) and cut from the Coomassie blue-stained gels into three portions according to their molecular weights (10–35 kDa, 35–70 kDa, and 70–180 kDa). Then the In-Gel proteins were digested and analyzed using the HPLC-Orbitrap-ELite Mass Spectrometer (Thermo Fisher Scientific) as previously described [23].

## 2.11 | Chromatin immunoprecipitation (ChIP) assay

The ChIP assay was performed using antibodies against human JUP, HDAC1, HIF2 $\alpha$ , p300, and H3K27ac as previously described [21]. The precipitated DNA was subjected to qPCR using primers described in Supplementary Table S1. Sonicated DNA was normalized for each sample of cells before immunoprecipitation.

## 2.12 | Colony formation, proliferation, migration, and invasion assays

Colony formation was measured two weeks after seeding 1000 cells per well in 6-well plates. Cell proliferation was measured using the Cell Counting Kit-8 (CCK-8) assay (Dojindo Laboratories, Kumamoto, Japan) according to the manufacturer's instructions. Migration and invasion assays were conducted using uncoated and Matrigel-coated Transwell® inserts (Corning, NY, USA) according to the manufacturer's instructions. At 12–24 h after the cell seeding into Transwell® inserts, migrating and invading cells were stained with 0.5% crystal violet solution and imaged with a microscope.

## 2.13 | Animal experiments

For the subcutaneous xenograft model,  $5 \times 10^6$  cells in 100  $\mu\text{L}$  phosphate-buffered saline (PBS) were injected subcutaneously in 7-week-old male BALB/c nude mice which were purchased from Beijing Huafukang Biotechnology (Beijing, China). Tumor volume was measured with calipers weekly and calculated according to the formula: volume =  $0.5 \times \text{length} \times \text{height} \times \text{width}$ .

For the tail intravenous injection assay,  $5 \times 10^6$  cells in 100  $\mu\text{L}$  PBS were injected into the tail vein of nude mice. The number and volume of metastases were examined weekly by an *in vivo* imaging system from day 28 after cell injection. All experiments were approved by the Animal Care and Use Committee of Tongji Medical College of Huazhong University of Science and Technology.

## 2.14 | The cancer genome atlas (TCGA) analysis

TCGA data of mRNA expression levels and clinical characteristics were downloaded from an integrated TCGA Pan-Cancer Clinical Data Resource [24]. Hypoxia scores for TCGA patients were calculated by Bhandari *et al.* [25] using the method developed by Ragnum *et al.* [26]. Kaplan-Meier analyses were conducted using GraphPad Prism (San Diego, CA, USA). The clinical characteristics of patients with different JUP expression levels were compared by using two-tailed chi-square test with the SPSS 20 software (SPSS Inc., Chicago, IL, USA). A *P* value <0.05 was considered significant.

## 2.15 | RNA sequencing and differential gene expression analysis

RNA sequencing of 786-O cells stably expressing sh-JUP or sh-LacZ was performed by Ouyi Biomedical Technology (Shanghai, China). The transcriptome of oligo-dT enriched mRNA was sequenced using HiSeqTM 2500 (Illumina, Watertown, MA, USA). Differential gene expression was determined by the R package edgeR [27] using Trimmed Mean of M-values (TMM) normalization.

# 3 | RESULTS

## 3.1 | Identification of JUP as an HIF2 $\alpha$ -associated protein

We first screened interaction proteins of HIF2 $\alpha$  using AP-MS. These experiments identified not only VHL, ARNT,

Egl-9 family hypoxia-inducible factor 1 (EGLN1) and Cullin 2 (CUL2), which were expected, but also several unreported proteins including JUP (data not shown). For validation, Flag-HIF2 $\alpha$  was co-expressed with HA-tagged JUP in HEK293T cells, and results showed HA-JUP efficiently co-precipitated with Flag-HIF2 $\alpha$  in HEK293T cells (Figure 1A and B). Additionally, bacterially expressed GST-JUP associated with Flag-HIF2 $\alpha$  (Figure 1C), indicating that HIF2 $\alpha$  directly interacted with JUP. Furthermore, endogenous JUP and HIF2 $\alpha$  co-precipitated in 786-O and OSRC-2 cells (Figure 1D). Given that both HIF1 $\alpha$  and HIF2 $\alpha$  sharing many common interaction proteins (e.g.,  $\beta$ -catenin [15] and c-Myc [28]), we examined whether JUP also binds to HIF1 $\alpha$ . As expected, Co-IP assays showed that EGFP-HIF1 $\alpha$  was co-precipitated efficiently with endogenous JUP (Figure 1E). These results indicate that JUP associates with both HIF1 $\alpha$  and HIF2 $\alpha$ .

## 3.2 | Identification of domains for JUP-HIF2 $\alpha$ interaction

Next, we determined the structural domains required for HIF2 $\alpha$ -JUP interaction. A series of truncated HIF2 $\alpha$  constructs were co-expressed with HA-JUP in HEK293T cells for AP and analysis. As shown in Figure 1F, the Per-Arnt-Sim (PAS) and PAS-associated C-terminal (PAC) regions (spanning amino acids 84–347) and the inhibitory (IH) domain of HIF2 $\alpha$  were sufficient for interaction with JUP. Similarly, JUP truncations were co-expressed with Flag-HIF2 $\alpha$ , revealing that both the N- and C-terminal domains of JUP were sufficient for HIF2 $\alpha$  interaction (Figure 1G).

## 3.3 | JUP expression in ccRCC tissues

JUP is a member of the Armadillo protein family and is a structural and functional homolog of  $\beta$ -catenin. Previous studies have indicated that JUP with diverse functions are involved in human cancer [29–35]. We next assessed the role of JUP expression on renal cancer development and progression. Twelve specimens of ccRCC tissues with adjacent normal tissues were collected to examine the mRNA levels of JUP by qPCR. JUP was significantly downregulated in these ccRCC samples compared with the corresponding adjacent normal tissues (Figure 2A). We also evaluated the protein level of JUP in 5 specimens of ccRCC, 4 of which showed low expression of JUP protein (Figure 2B). We further JUP expression in a ccRCC tissue array from Shanghai Superchip (Supplementary Fig. S1, Figure 2C). Weak JUP staining was detected in 13 (86.7%) of 15 ccRCC tissues. In contrast, most normal tissues (14 of 15) exhibited strong JUP staining.

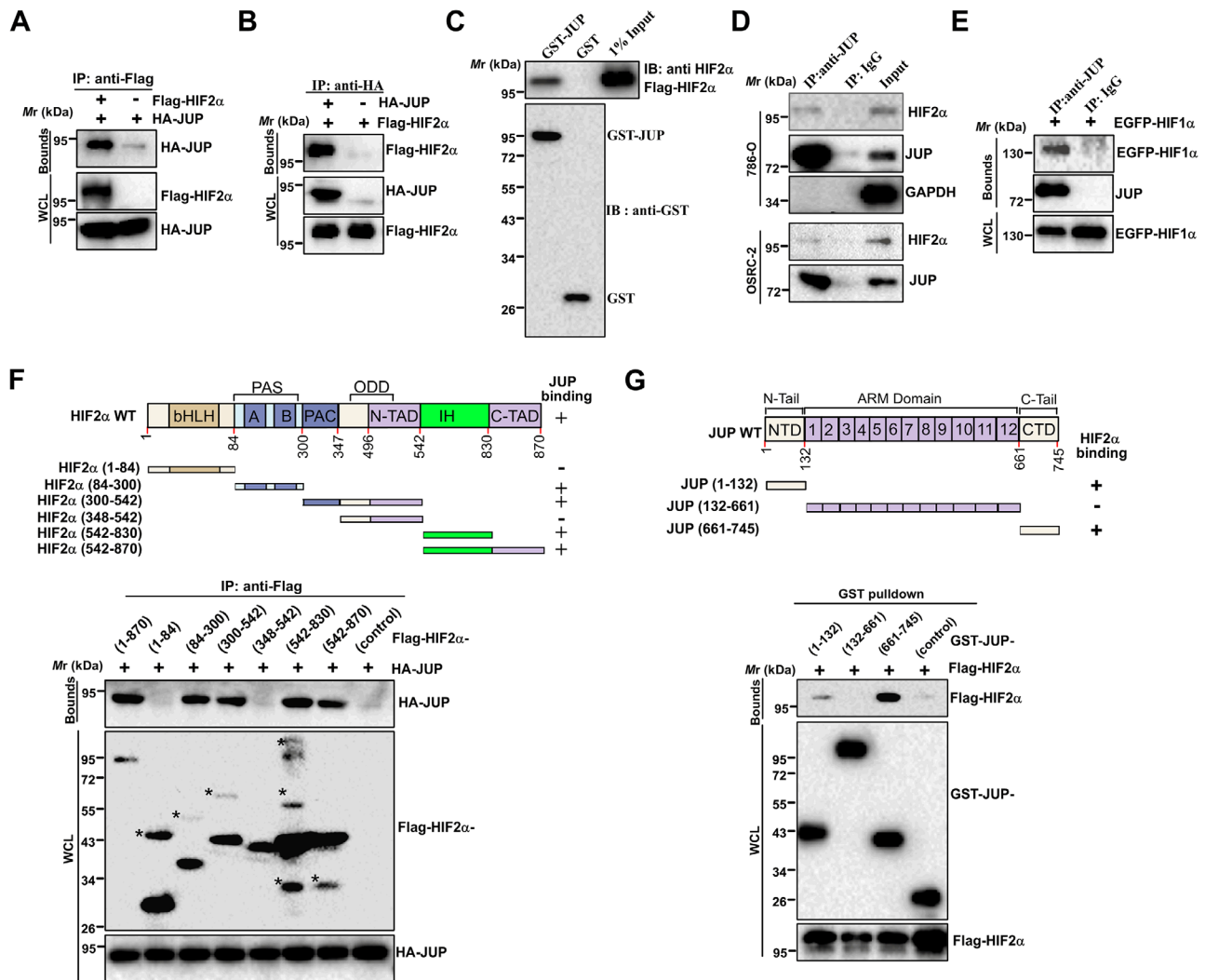


**FIGURE 1** JUP interaction with HIF2 $\alpha$ . A and B, HEK293T cells were transfected with Flag-HIF2 $\alpha$  and HA-JUP. The cell lysates were immunoprecipitated with anti-Flag (A) or anti-HA antibody (B), and co-immunoprecipitated proteins were detected by Western blotting analysis with anti-HA or anti-Flag antibody, respectively. C, Purified GST or GST-JUP was incubated with Flag-HIF2 $\alpha$ -expressing 786-O lysates and precipitated with glutathione-agarose beads. Pulled-down Flag-HIF2 $\alpha$  proteins by GST-JUP were detected by immunoblotting with the HIF2 $\alpha$  antibody. Purified GST or GST-JUP was visualized by Western blotting analysis using the GST antibody. D and E, 786-O cells were harvested and subjected to endogenous Co-IP analysis with JUP antibody. Rabbit IgG was used as a control. F, Schematic diagram of the various domains and relevant mutant fusion expression constructs of HIF2 $\alpha$  (upper). HA-JUP and Flag-HIF2 $\alpha$  full-length and deletion mutants were ectopically expressed in HEK293T cells, followed by Flag-immunoprecipitation and immunoblotting with HA antibody. Inputs are shown in the bottom panels. G, GST pull-down assay detecting the regions of JUP that bind to HIF2 $\alpha$ . Schematic diagram of the various domains and relevant mutant fusion expression constructs of JUP (upper). Flag-HIF2 $\alpha$  and GST-JUP deletion mutants were ectopically expressed in HEK293T cells, followed by Western blotting analysis of Flag-HIF2 $\alpha$  pulled down by GST or GST-JUP fusion proteins. Inputs are shown in the bottom panels. Abbreviations: HIF, hypoxia-inducible factor; JUP, junction plakoglobin; bHLH, basic helix-loop-helix; PAS, Per-Arnt-Sim; PAC, PAS-associated C-terminal; ODD, oxygen-dependent degradation; N-TAD, N-terminal transactivation domain; C-TAD, C-terminal transactivation domain; IH, inhibitory domain; ARM, armadillo; NTD, N-terminal domain; CTD, C-terminal domain; GST, glutathione-S-transferase; Co-IP, co-immunoprecipitation

We further examined JUP expression in a TCGA cohort and found it was significantly downregulated in ccRCC tumors compared with normal tissues (Figure 2D). Additionally, JUP expression differed significantly in patients according to pathologic grade ( $P < 0.001$ ), TNM stage ( $P < 0.001$ ), and distant metastasis ( $P = 0.041$ ) (Supplemen-

tary Table S2). We also found that JUP was significantly decreased in stages III and IV ccRCC compared with stages I and II tissues (Figure 2E). Furthermore, Kaplan-Meier survival analysis demonstrated patients with low JUP expression had significantly poorer OS, disease-specific survival, and progression-free survival compared to those

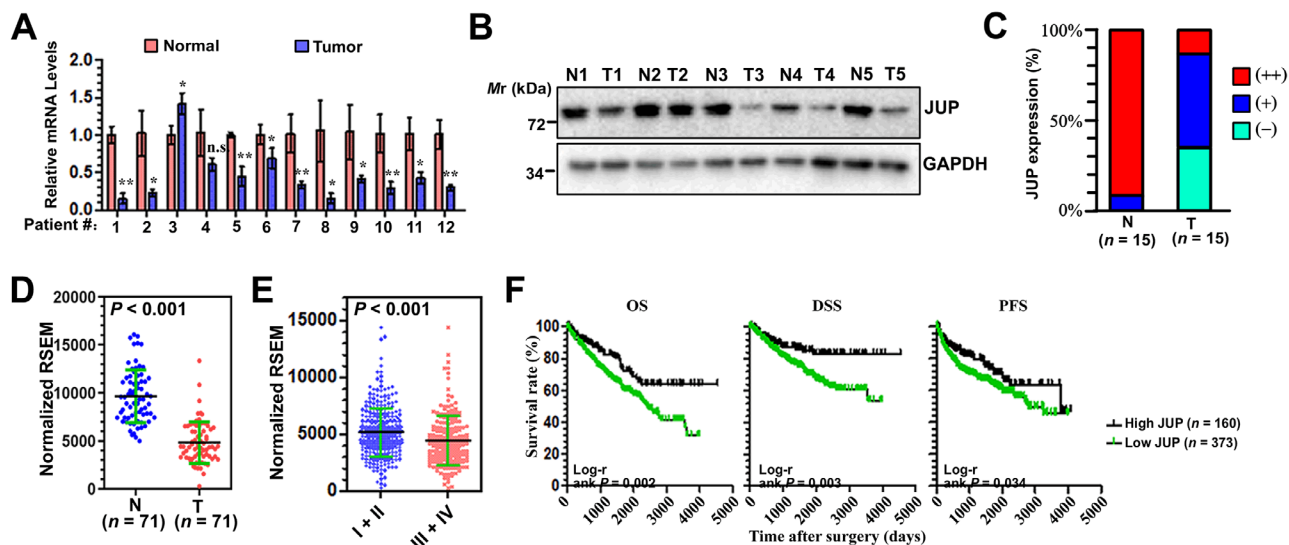


**FIGURE 2** JUP expression in ccRCC tissues. A, qPCR analysis of JUP expression in 12 specimens of ccRCC and adjacent normal tissues. B, JUP protein levels in the paired tumor (T) and adjacent normal (N) tissues. C, Quantification of JUP protein levels in a tissue array containing 15 specimens of ccRCC and adjacent normal tissues. JUP levels were classified into three grades (negative [-], weak positive [+], and strong positive [++]) according to results from immunofluorescence staining. D, JUP expression was significantly downregulated in ccRCC tumors compared with normal tissues. E, There was low expression of JUP in stage III and IV ccRCCs. F, Kaplan–Meier analysis identified that patients with low JUP expression exhibited shorter survival compared to those with high JUP expression. Abbreviations: RSEM, RNA-Seq by Expectation-Maximization; OS, overall survival; DSS, disease-specific survival; PFS, progression-free survival; JUP, junction plakoglobin; ccRCC, clear cell renal cell carcinoma

with high JUP expression (Figure 2F), indicating JUP might be an independent prognostic factor for ccRCC survival.

### 3.4 | The effects of JUP on the proliferation and metastasis of RCC cells

Next, we examined the possible role of JUP in ccRCC progression. We first stably expressed JUP in ACHN and 786-O cells and found that JUP inhibited colony formation (Figure 3A). Additionally, JUP suppressed the migration of these cells in a wound healing assay (Figure 3B). Consistent with the wound healing results, overexpression of JUP also inhibited the migration and invasion of these cells in the transwell assays (Figure 3C). Together, these results suggest that JUP may function as a tumor suppressor in ccRCC.

Next, we determined whether JUP depletion could promote tumor growth in a xenograft mouse model. Although JUP knockdown (JUP-KD) had no effect on the *in vitro* growth of ACHN and 786-O cells (Supplementary Fig. S2), tumors from subcutaneously transplanted ACHN cells with stable knockdown of JUP grew more rapidly compared with the controls (Figure 3D–F). Immunohistochemical staining showed that the expression of Ki-67, a cell proliferation marker, was significantly increased

in JUP-KD tumors compared with sh-LacZ tumors (Figure 3G), suggesting increased cell proliferation in tumors by JUP-KD.

Finally, we studied the effect of JUP-KD on RCC cell metastasis to other parts of the body. In intravenous injection assay with EGFP quantitative imaging, we noticed that the mice injected with JUP-KD cells had a marked increase in fluorescence signal compared with those injected with control cells. Of the nine mice injected with JUP-KD cells, five developed detectable lesions, as observed in a live-animal imaging system, whereas only one mouse injected with sh-LacZ cells developed detectable lesions. Representative fluorescence images at eight weeks post-injection showed that more metastasis occurred in the leg and lung after JUP-KD (Figure 3H). Moreover, the overall survival (OS) curves showed the JUP-knockdown group had a worse prognosis than the sh-LacZ group (Figure 3I). Together, these findings indicate JUP is a potent tumor suppressor that inhibits RCC progression.

### 3.5 | JUP plays a key role in regulating the HIF2 $\alpha$ transcriptional activity

We next determined whether JUP affected the transactivation of HIF2 $\alpha$ . Using 6xHRE-driven luciferase reporter, our results showed JUP decreased the transcriptional activity

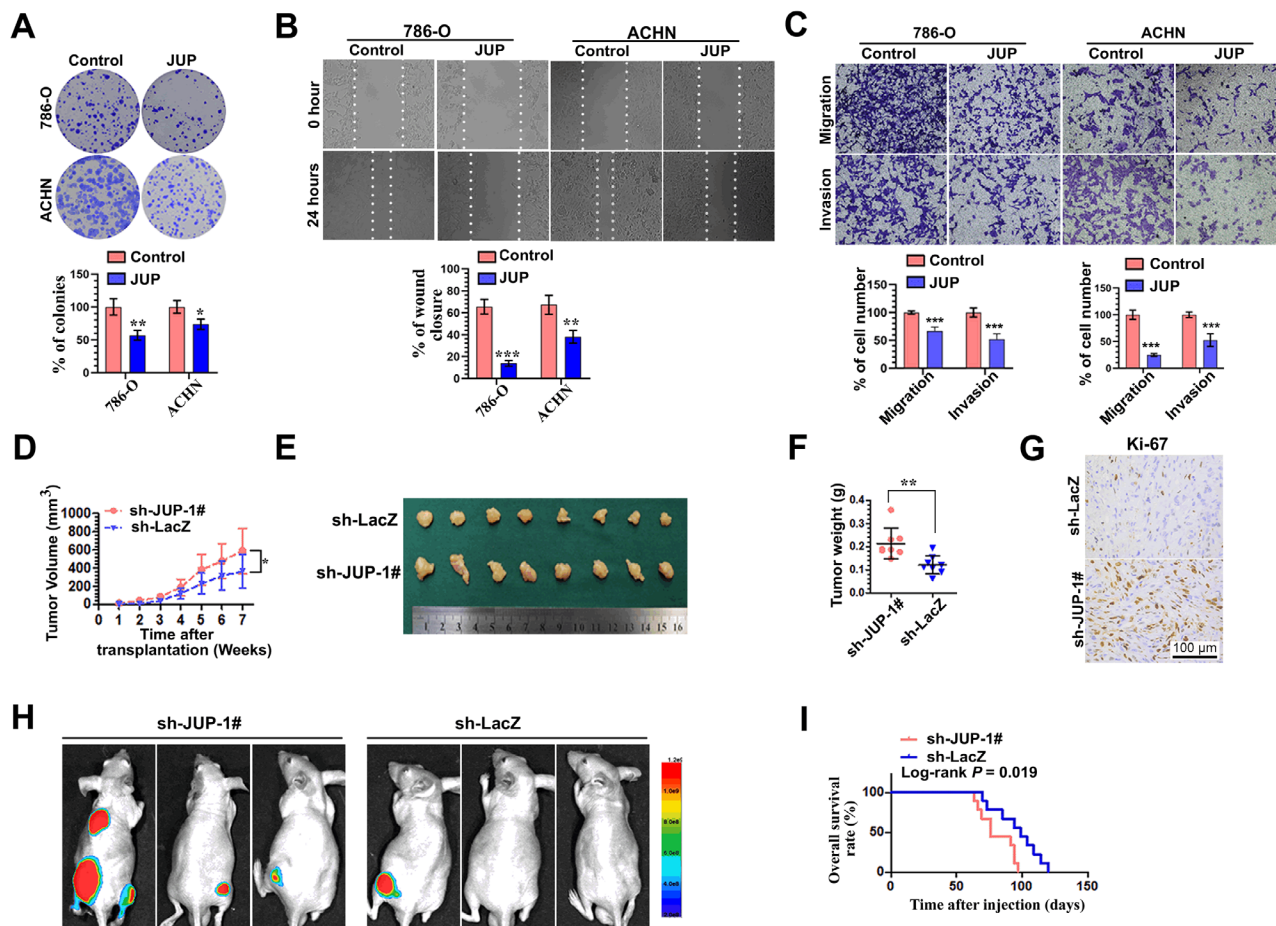


**FIGURE 3** JUP suppresses renal cancer proliferation and metastasis. **A**, JUP inhibited the proliferation of ACHN and 786-O cells. The cells were stably transfected with a vector control or JUP and analyzed by colony formation assays. Images of the whole plate are shown in the upper panels, and the number of colonies was quantified in the lower panels. Data are plotted as the mean  $\pm$  SD of three independent experiments. **B**, Wound healing assay of ACHN and 786-O cells expressing a vector control or JUP. Data are plotted as the mean  $\pm$  SD of 3 independent experiments. **C**, Migration and invasion assays for RCC cells. Migrated and invaded cells from each treatment group were counted in five random images. Three experiments were conducted, and a mean  $\pm$  SD of relative cell numbers was plotted. **D–F**, ACHN cells stably expressing sh-JUP-1# and sh-LacZ (control) were subcutaneously injected into the left and right flanks of nude mice as indicated. The tumor volumes were measured every week after transplantation (**D**), and the macroscopic appearances (**E**) and weight (**F**) of tumors at week 7 post-transplantation are shown. **G**, Representative hematoxylin and eosin-stained xenograft tumors corresponding to week 7 after injection. **H**, Metastatic colonization was assessed by fluorescence small-animal imaging system. **I**, Kaplan-Meier survival analysis for mice injected by the tail vein with sh-LacZ ( $n = 9$ ) or sh-JUP ACHN cells ( $n = 9$ ). \* $P < 0.05$ , \*\* $P < 0.01$ , and \*\*\* $P < 0.001$ . Abbreviations: JUP, junction plakoglobin; RCC, renal cell carcinoma

of both transfected and endogenous HIF2 $\alpha$  in HEK293T and 786-O cells, respectively (Figure 4A and B). Moreover, when JUP fragments were expressed, the N-terminal of JUP decreased the transactivation of HIF2 $\alpha$ , whereas the C-terminal of JUP had the opposite effect (Figure 4C). We also observed JUP-KD resulted in upregulation of HIF2 $\alpha$  target genes in both 786-O and OSRC-2 cells (Figure 4D and E). To confirm the role of JUP in HIF2 $\alpha$  activation, we performed genome-wide expression profiling of 786-O cells after JUP-KD (Supplementary Table S3). Gene Ontology analysis revealed JUP regulated cell communication, adhesion, and growth and ion transport genes (Supplementary Table S4). Additionally, biological

pathway analysis demonstrated JUP repressed distinct pathways including the vascular endothelial growth factor (VEGF)/VEGF receptor, HIF1 $\alpha$ , and HIF2 $\alpha$  (Figure 4F and Supplementary Table S5). Furthermore, the overlapping data from JUP and HIF2 $\alpha$  transcriptome analysis revealed that 85 HIF2 $\alpha$ -activated genes were repressed by JUP (Figure 4G), indicating JUP inhibits the expression of a subset of HIF2 $\alpha$  target genes. qPCR further validated six differentially expressed genes in two JUP-stable knockdown cell lines (Figure 4H). Given that HIF2 $\alpha$  plays an important role in the adaptive cellular response to hypoxia in ccRCC, we examined the correlation between JUP expression and hypoxia gene signature in the TCGA cohort. Consistent



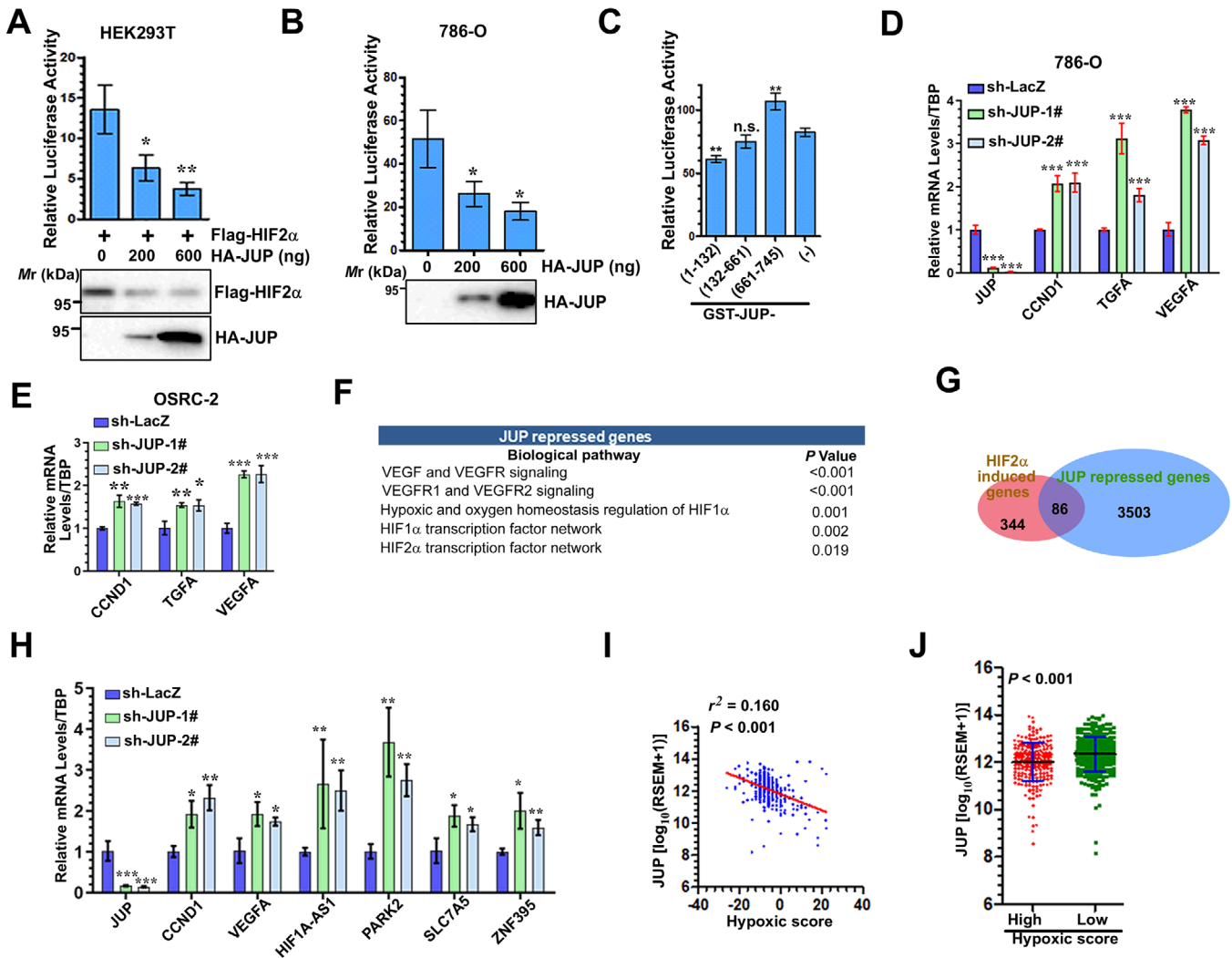


**FIGURE 4** JUP negatively regulates the activity of HIF2 $\alpha$  in RCC cells. **A**, The relative luciferase activity and Western blotting analysis of HEK293T cells transfected with Flag-HIF2 $\alpha$  (100 ng) with the indicated doses of HA-JUP (0, 200, or 600 ng). **B**, JUP inhibits 6 $\times$ HRE-driven luciferase activity in VHL-null 786-O cells (expressing HIF2 $\alpha$ , but not HIF1 $\alpha$ ). **C**, The N-terminal of JUP is required for the transcriptional inhibition of HIF2 $\alpha$ . 786-O cells were transfected with 6 $\times$ HRE-driven luciferase reporter and pGL4.73 along with serial deletion mutants of GST $\eta$ tagged JUP or GST (control). **D** and **E**, qPCR showed that JUP-KD enhanced *VEGFA*, *TGFA*, and *CCND1* transcription in 786-O cells (**D**) and OSRC-2 cells (**E**) expressing sh-JUP-1#, sh-JUP-2#, or sh-LacZ (control). **F**, Biological pathway analysis of JUP repressed genes showed enrichment of the HIF pathway and VEGF signaling in 786-O cells. **G** Venn diagram showing the intersection of HIF2 $\alpha$ -activated and JUP-repressed transcriptomes revealed 86 co-regulated genes. **H**, Validation of RNA-seq results by qPCR of six genes was performed. The experiments were repeated at least three times, and the results are shown as the mean  $\pm$  SD and were analyzed by the unpaired two-tailed Student's *t*-test ( $n = 3$ ). **I**, Scatterplot of hypoxic signature score against gene expression levels of JUP in ccRCC samples from a TCGA cohort. **J**, JUP was highly expressed in ccRCC patients with a low hypoxic score. \* $P < 0.05$ , \*\* $P < 0.01$ , and \*\*\* $P < 0.001$ . Abbreviations: TBP, TATA box binding protein; JUP, junction plakoglobin; RCC, renal cell carcinoma; qPCR, quantitative polymerase chain reaction; JUP-KD, JUP knockdown; *n.s.*, not significant

with the negative regulation of HIF2 $\alpha$  activity by JUP, we found a negative correlation between JUP mRNA levels and hypoxia gene signature in ccRCC samples ( $r^2 = 0.160$ ,  $P < 0.001$ ; Figure 4I), but not in other cancer types (data not shown). Furthermore, hypoxia grading in ccRCC samples revealed JUP was significantly decreased in the ccRCC tissues with a high hypoxic signature (Figure 4J).

### 3.6 | Mechanism of regulation of HIF2 $\alpha$ stability by JUP

HIF2 $\alpha$  stability is critical for inducing the expression of HIF2 $\alpha$  target genes, such as vascular endothelial growth factor A (*VEGFA*) [5] and zinc finger protein 395 (*ZNF395*) [36], so we tested whether JUP regulates HIF2 $\alpha$

stability. When JUP was overexpressed, we found endogenous HIF2 $\alpha$  protein level was decreased (Figure 5A). The HIF2 $\alpha$  decrease induced by JUP overexpression was reversed by the proteasome inhibitor MG132 (Figure 5B). In parallel, shRNA-induced downregulation of JUP increased HIF2 $\alpha$  levels in VHL-proficient ACHN and SN12-PM6 cells (Figure 5C and D). Additionally, JUP overexpression reduced the half-life of endogenous HIF2 $\alpha$  in a cycloheximide chase experiment (Figure 5E and F), whereas JUP-KD led to the opposite effect (Figure 5G and H). Next, we examined whether JUP regulates HIF2 $\alpha$  stability by promoting HIF2 $\alpha$  ubiquitination. We found overexpression of JUP increased HIF2 $\alpha$  ubiquitination (Figure 5I). This indicates JUP binds to and promotes HIF2 $\alpha$  ubiquitination. Next, we examined whether promotion of HIF2 $\alpha$  ubiquitination by JUP required a functional VHL protein. Overexpression of JUP in VHL-deficient 786-O cells had little effect on endogenous HIF2 $\alpha$  levels (Supplementary Fig. S3A). In addition, the inhibitory effect of JUP on HIF2 $\alpha$  levels was restored by co-expression of VHL WT but not by the VHL (Y98N) mutant (Supplementary Fig. S3B), indicating VHL is required for this effect. Consistent with this observation, overexpression of JUP had little effect on exogenously produced hydroxylation-defective mutant HIF2 $\alpha$  (P405A/P531A) levels (Supplementary Fig. S3C). Furthermore, downregulation of JUP in VHL-null 786-O cells with shRNA resulted in no measurable effects on HIF2 $\alpha$  stability (Supplementary Fig. S3D). This indicated JUP regulates HIF2 $\alpha$  ubiquitination in a VHL-dependent way. Therefore, we investigated whether JUP interact with VHL. Endogenous JUP protein was observed after incubation with GST-VHL (Figure 5J). Co-IP assays showed that Flag-VHL efficiently co-precipitated with endogenous and exogenous JUP in HEK293T cells (Figure 5K and L). We next tried to identify the interacting site of JUP with VHL. Co-IP results indicate that VHL co-precipitated with the N-terminal domains of JUP (Figure 5M). Then we examined the possibility that JUP facilitates the binding of VHL to HIF2 $\alpha$ . Ectopically expressed JUP was found to strengthen VHL-HIF2 $\alpha$  interaction (Figure 5N). Taken together, these findings suggest that JUP promotes the ubiquitination of HIF2 $\alpha$  by facilitating the VHL-HIF2 $\alpha$  interaction.

### 3.7 | JUP regulates HIF2 $\alpha$ transactivation through the recruitment of HDACs

Because JUP interacts with the HIF2 $\alpha$  PAS domain, which is required for heterodimerization with ARNT, we speculated that JUP may interfere with HIF2 $\alpha$ -ARNT interaction. To test this hypothesis, Co-IP assays using HIF2 $\alpha$ , JUP, and ARNT constructs were performed in HEK293T

cells. Unexpectedly, JUP overexpression had a minimal effect on HIF2 $\alpha$ -ARNT interactions (Supplementary Fig. S4A). Instead, the JUP-ARNT interaction was independent of HIF2 $\alpha$  (Supplementary Fig. S4B). Therefore, we hypothesized that JUP serves as a co-repressor to inhibit transactivation of the HIF2 $\alpha$ /ARNT heterodimer.

We noticed that JUP also inhibited the transcriptional activity of endogenous HIF2 $\alpha$  in VHL-null 786-O cells (Figure 4), suggesting an alternate, VHL-independent mechanism for JUP-mediated inhibition of HIF2 $\alpha$ . Overexpression of JUP still repressed the transcriptional activity of the HRE reporter induced by HIF2 $\alpha$  mutant (P405A and P531A double mutant [DM]) (Supplementary Fig. S5). As expected, JUP inhibition of HIF2 $\alpha$ -DM signaling was weaker than WT HIF2 $\alpha$  signaling for the HRE luciferase reporter (Supplementary Fig. S5), indicating JUP may inhibit HIF2 $\alpha$  signaling in both VHL-dependent and VHL-independent manners.

Considering that HDACs usually act as co-repressors for many transcription factors and given HIF2 $\alpha$  also interacted with HDAC1/2 (data not shown), we determined whether JUP interacts with HDAC1/2. To this end, we performed Co-IP experiments with Flag-tagged-HDAC1/2 to test the association of HDAC1/2 with JUP and HIF2 $\alpha$  and revealed that endogenous JUP and HIF2 $\alpha$  associated with both HDAC1 and HDAC2 in 786-O cells (Figure 6A). We next tried to identify the JUP site for HDAC1 binding. Co-IP analyses showed that the JUP C-terminus is responsible for binding HDAC1 (Figure 6B). Because the JUP sites for HDAC1 and HIF2 $\alpha$  binding are not identical, JUP might regulate the HIF2 $\alpha$ -HDAC1/2 interaction. To test this possibility, we co-expressed HDAC1/2 with or without JUP and performed Co-IP analysis. JUP overexpression strengthened both HIF2 $\alpha$ -HDAC1 and HIF2 $\alpha$ -HDAC2 interactions (Figure 6C). To further understand the JUP-mediated enhancement of the HIF2 $\alpha$ -HDAC1/2 interaction, we investigated whether JUP directly interacted with HDAC1 or HDAC2 independent of HIF2 $\alpha$ . Flag-HDAC1/2 proteins were observed after incubation with GST-JUP (Figure 6D), indicating JUP can recruit HDAC1/2 without HIF2 $\alpha$ .

These studies suggest JUP may act as a corepressor by recruiting HDACs to HIF2 $\alpha$ .

We next performed the ChIP assays to test whether JUP affects HDAC1/2 binding to the *VEGFA* and *ZNF395* loci, two well-known HIF2 $\alpha$ -responsive genes upregulated upon JUP depletion. HIF2 $\alpha$  bound the *VEGFA* promoter and *ZNF395* enhancer sites (Figure 6E). ChIP analysis indicated that the binding of JUP and HDAC1 to the *VEGFA* promoter and *ZNF395* enhancer were decreased by HIF2 $\alpha$  depletion (Figure 6F and G); this interaction is likely HIF2 $\alpha$ -dependent. By contrast, HIF2 $\alpha$  binding to these sites was unchanged when either JUP or HDAC

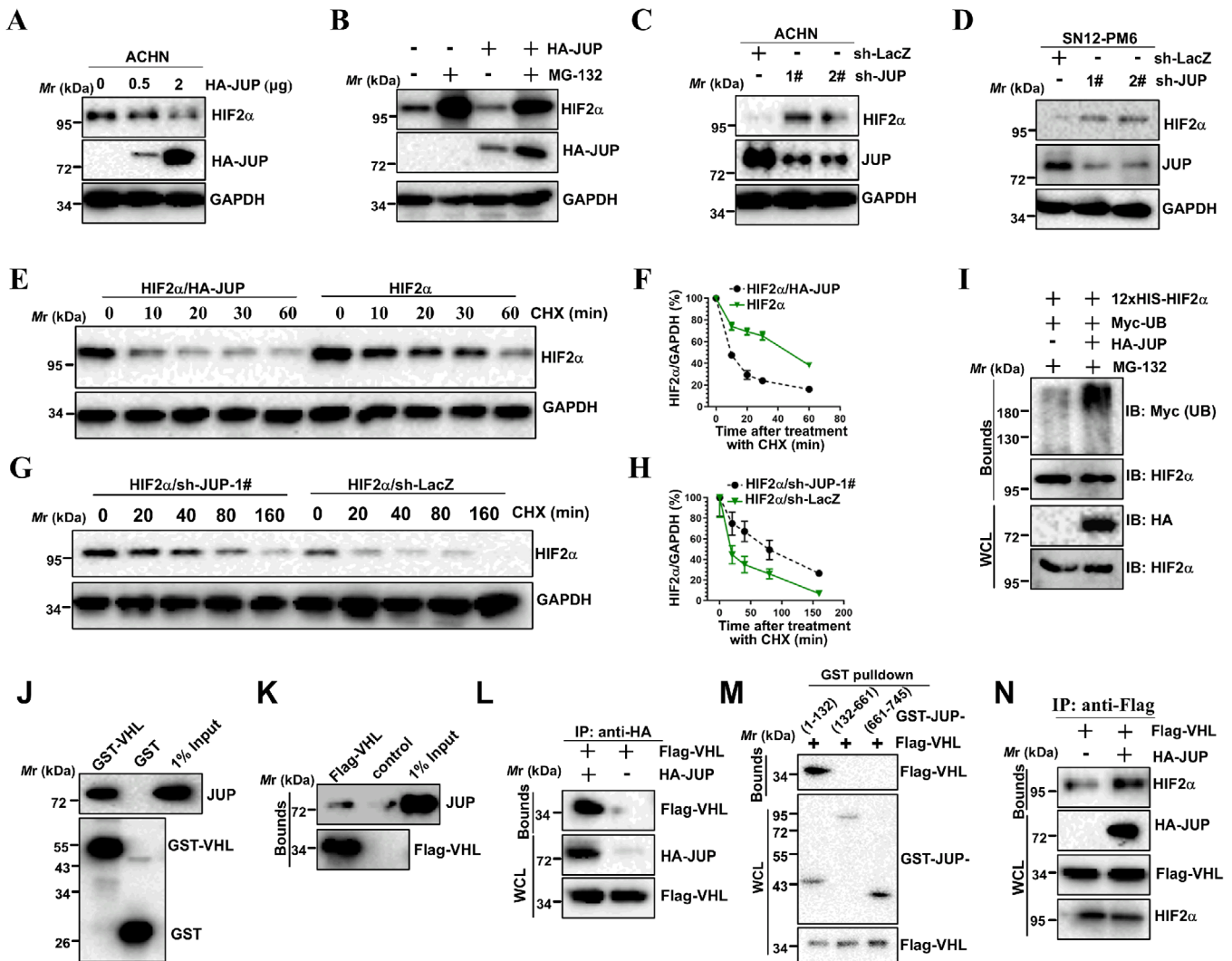


**FIGURE 5** JUP promotes HIF2 $\alpha$  ubiquitination and degradation by facilitating HIF2 $\alpha$ -VHL interaction. **A**, JUP affected HIF2 $\alpha$  protein levels in ACHN cells. ACHN cells were transfected with HA-JUP (0, 0.5, or 2  $\mu$ g) plasmids. Cell lysates were subjected to SDS-PAGE followed by immunoblotting with anti-HIF2 $\alpha$ , anti-HA, or anti-GAPDH antibody. **B**, Downregulation of HIF2 $\alpha$  level by JUP was reversed by MG132. Cells transfected with HA-JUP were left untreated or were treated with MG132, and HIF2 $\alpha$  level was examined by Western blotting. **C** and **D**, ACHN and SN12-PM6 cells were stably transfected with JUP shRNAs, and the HIF2 $\alpha$  level was examined. **E**, ACHN cells stably expressing HIF2 $\alpha$ /LacZ shRNA or HIF2 $\alpha$ /JUP shRNA were treated with 100  $\mu$ mol/L cycloheximide and harvested at the indicated time points to examine HIF2 $\alpha$  levels. **F**, Quantification of HIF2 $\alpha$  protein expression level in panel **E** shows the effect of JUP on HIF2 $\alpha$  stability. **G**, ACHN cells stably expressing HIF2 $\alpha$ /HA-JUP or HIF2 $\alpha$  were treated with 100  $\mu$ mol/L cycloheximide and harvested at the indicated time points to examine HIF2 $\alpha$  levels. **H**, Quantification of HIF2 $\alpha$  protein expression level shown in panel **G**. **I**, JUP enhanced HIF2 $\alpha$  ubiquitination in ACHN cells. Cells were stably transfected with the indicated plasmids and then treated with MG132 (10  $\mu$ g/mL) for 6 h. Ubiquitinated proteins were pulled down by Ni-NTA agarose under denaturing conditions, and then analyzed by Western blotting with Myc, HIF2 $\alpha$ , and HA antibodies. **J**, GST pull-down assay detecting JUP-VHL interaction. GST or GST-VHL purified from *E. coli* was incubated with 786-O cell lysates and precipitated with glutathione-agarose beads, followed by Western blotting analysis of anti-JUP. **K**, Co-IP of endogenous JUP from extracts of 786-O cells expressing Flag-VHL. **L**, Co-IP of HA-JUP with VHL in 786-O cells. The 786-O cells transfected with HA-JUP and Flag-VHL were subjected to Co-IP with anti-HA antibody. **M**, GST pull-down assay detecting the regions of JUP that bind to VHL. Flag-VHL and GST-JUP deletion mutants were ectopically expressed in HEK293T cells, followed by Western blotting analysis of Flag-VHL pulled down by GST-JUP fusion deletion mutants. Inputs are shown in the bottom panels. **N**, JUP promoted the HIF2 $\alpha$ -VHL interaction. 786-O cells were co-transfected with Flag-VHL (0.6  $\mu$ g) and HA-JUP (0 or 1  $\mu$ g) plasmids. Endogenous HIF2 $\alpha$  co-immunoprecipitated with Flag antibody. Abbreviations: CHX, cycloheximide; JUP, junction plakoglobin

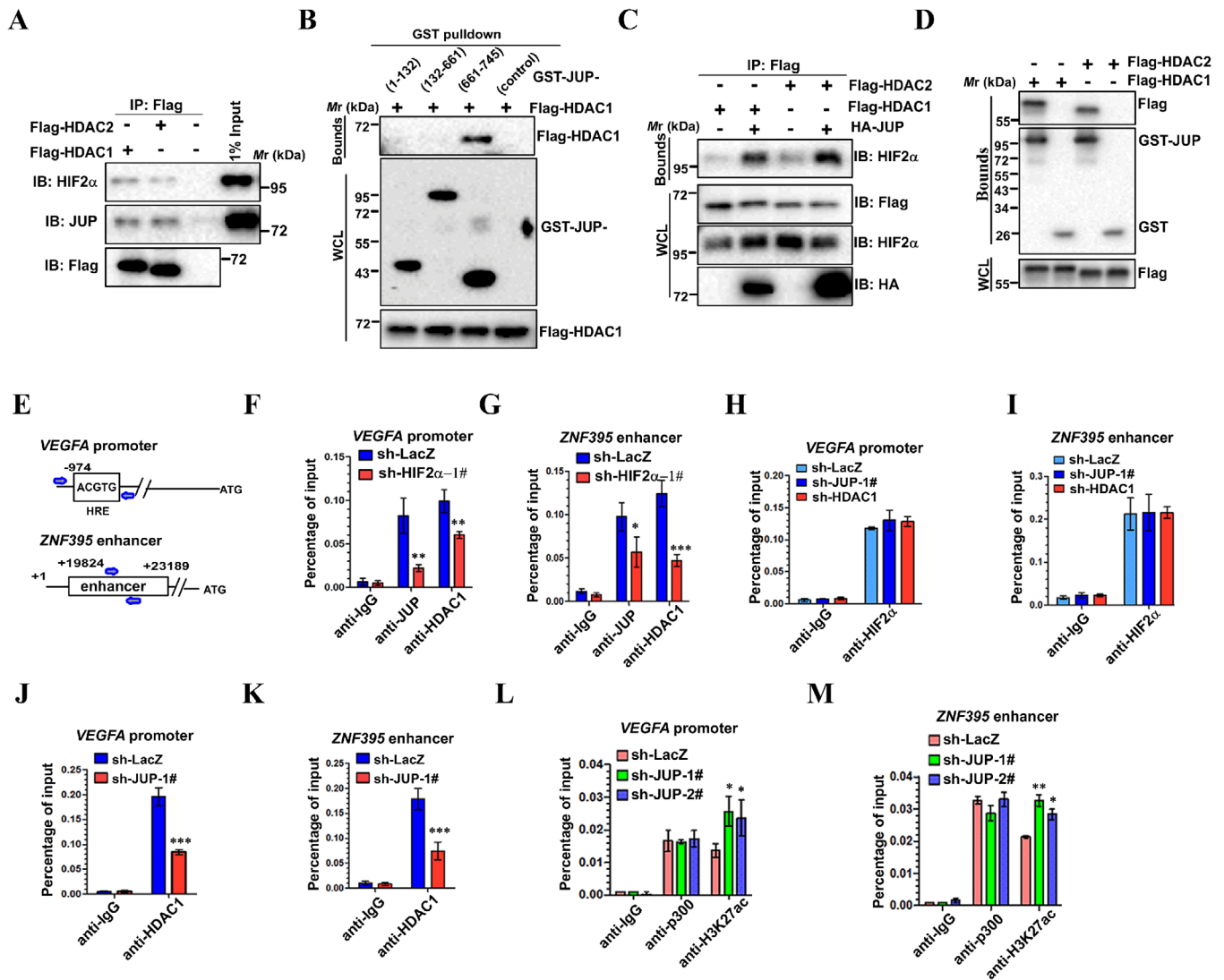


**FIGURE 6** Recruitment of HDAC1/2 to HIF2 $\alpha$  by JUP decreases H3K27ac levels at HIF2 $\alpha$ -binding sites in RCC cells. **A**, Endogenous HIF2 $\alpha$  and JUP co-immunoprecipitated with Flag-HDAC1/2 in 786-O cells. 786-O cells stably expressing Flag-HDAC1 or Flag-HDAC2 were lysed and immunoprecipitated with anti-Flag antibody. **B**, GST pull-down assay detecting the regions of JUP that bind to HDAC1. Flag-HDAC1 and GST-JUP deletion mutants were ectopically expressed in HEK293T cells, followed by Western blotting analysis of Flag-HDAC1 pulled down by GST or GST-JUP deletion mutants. Inputs are shown in the bottom panels. **C**, JUP promoted both HDAC1 and HDAC2 binding to HIF2 $\alpha$ . 786-O cells were co-transfected with Flag-HDAC1 or Flag-HDAC2 (0.6  $\mu$ g) and HA-JUP (0 or 1  $\mu$ g) plasmids. Endogenous HIF2 $\alpha$  co-immunoprecipitated with Flag antibody. **D**, GST pull-down assay detecting JUP-HDAC1/HDAC2 interaction. **E**, Schematic diagram of regulatory regions in *VEGFA* promoter and *ZNF395* enhancer shows the HIF DNA-binding sites. Numbers indicate nucleotides with the transcription start site indicated by +1. **F** and **G**, ChIP analysis with anti-JUP or anti-HDAC1 antibody in WT- or HIF2 $\alpha$ -specific depleted 786-O cells. Precipitated DNAs were quantified by qPCR of fragments around the HIF-binding site at the *VEGFA* promoter (**F**) and *ZNF395* enhancer (**G**). **H** and **I**, ChIP analysis with anti-HIF2 $\alpha$  antibody in WT-, JUP-, or HDAC1-specific depleted 786-O cells. Precipitated DNAs were quantified by qPCR of fragments around the HIF-binding site at the *VEGFA* promoter (**H**) and *ZNF395* enhancer (**I**). **J** and **K**, ChIP-qPCR validated the recruitment of HDAC1 by JUP at the *VEGFA* promoter (**J**) and *ZNF395* enhancer (**K**) in 786-O cells. **L** and **M**, ChIP-qPCR of p300 binding and H3K27ac enrichment at the *VEGFA* promoter (**L**) and *ZNF395* enhancer (**M**) in WT- or JUP-specific depleted 786-O cells. \* $P < 0.05$ , \*\* $P < 0.01$ , and \*\*\* $P < 0.001$ . Abbreviations: ZNF395, zinc finger protein 395; H3K27ac, histone H3K27 acetylation; ChIP, chromatin immunoprecipitation; JUP, junction plakoglobin; RCC, renal cell carcinoma

was depleted in 786-O cells, suggesting that HIF2 $\alpha$  binding to these sites is JUP- and HDAC1-independent (Figure 6H and I). As mentioned above, we demonstrated that JUP enhanced the HIF2 $\alpha$ -HDAC1 interaction. Thus, we asked whether the binding of HDAC1 to these sites is regulated by JUP. As expected, JUP depletion decreased binding of HDAC1 to HIF2 $\alpha$  target sites compared with the control (Figure 6J and K). Given that p300/CBP-mediated H3K27ac is a well-defined marker of active enhancers and promoters, we next tested whether JUP can regulate localization of p300 and H3K27Ac at these sites. Interestingly, we did not detect any change of p300 binding to these sites when JUP was knocked down (Figure 6L and M). However, the H3K27ac signals in these HIF2 $\alpha$ -binding sites were slightly increased upon JUP depletion (Figure 6L and M). Collectively, these data suggest JUP promotes recruitment of HDAC1 to deacetylation of H3K27 at HIF2 $\alpha$  target sites and further inhibits transcription of these target genes.

### 3.8 | JUP regulates RCC migration and invasion via HIF2 $\alpha$

As HIF2 $\alpha$  plays key roles at all stages of metastasis, we next investigated whether JUP affects cell migration and invasion by functionally repressing HIF2 $\alpha$ . The effects of JUP-KD on migration and invasion were partially reversed by concomitant HIF2 $\alpha$  knockdown (Figure 7A and B), suggesting the effects of JUP on cell migration and invasion are mediated, at least in part, through HIF2 $\alpha$ . As a control, knockdown of HIF2 $\alpha$  alone resulted in a marked decrease in migration and invasion (Figure 7B). Consistently, 786-O cells with HIF2 $\alpha$  and JUP co-silencing grew significantly slower than cells with JUP silencing alone (Figure 7C). In addition, cell migratory and invasive abilities were increased in HIF2 $\alpha$ -overexpressing cells, and further enhanced by JUP-KD (Figure 7D and E), again suggesting JUP is a potent tumor suppressor that inhibits HIF2 $\alpha$  function. Finally, we focused on the effects of JUP and mutant JUP ( $\Delta$ N/C, lacking both N- and C-terminal domains) on HIF2 $\alpha$ -mediated migration and invasion. Our result showed the migration and invasion activity were increased in HIF2 $\alpha$ -overexpressing cells, an effect that was partially reversed by the expression of full-length JUP, but not of mutant JUP (Figure 7F and G). Together, these data show JUP inhibits the HIF2 $\alpha$ -enhanced migration and invasion of RCC cells.

## 4 | DISCUSSION

In this study, we identified JUP as a novel HIF2 $\alpha$  binding partner, and found that HIF2 $\alpha$  signaling was inhibited

by the JUP protein. Importantly, the low expression of JUP occurred in clinical ccRCC samples and was correlated with enhanced hypoxia scores.

JUP, also named plakoglobin and  $\gamma$ -catenin, is a structural and functional homolog of  $\beta$ -catenin. The best-known function of these catenin proteins is to regulate cell-cell adhesion [37, 38]. There is crosstalk between  $\beta$ -catenin signaling and HIF signaling in cancers. The interaction of  $\beta$ -catenin with HIF1 $\alpha$  and HIF2 $\alpha$  has been observed in various cancer cells, and  $\beta$ -catenin can enhance both HIF1 $\alpha$ - and HIF2 $\alpha$ -mediated transcription [15, 39, 40]. However, HIF1 $\alpha$ - $\beta$ -catenin interaction dissociates transcription factor 4 from  $\beta$ -catenin and inhibited  $\beta$ -catenin activity, which is enhanced by the HIF2 $\alpha$ - $\beta$ -catenin interaction [15, 16, 39, 41]. The opposite effects of HIF1 $\alpha$  and HIF2 $\alpha$  on  $\beta$ -catenin signaling may be caused by the different domains of  $\beta$ -catenin responsible for the interactions with HIF1 $\alpha$  and HIF2 $\alpha$  [15, 39]. Here, we found JUP associates with HIF2 $\alpha$  through its N- and C-terminal transactivation domains, whereas only the N-terminal domain-truncated mutant decreased HIF2 $\alpha$  transactivation. Interestingly, it was reported that  $\beta$ -catenin binds to HIF2 $\alpha$  via its N-terminal domain (amino acids 1-259) [15], indicating the N-terminal domains of both JUP and  $\beta$ -catenin are critical for the regulation of HIF2 $\alpha$  function. We also found the C-terminal domain of JUP could interact with HIF2 $\alpha$ . However, when this domain was overexpressed in 786-O cells, HIF2 $\alpha$  transcriptional activity was enhanced. Solanas *et al.* [42] demonstrated the C-terminal domain of JUP interacts with the armadillo repeat domain and regulates the ability of this region to complex with other cofactors such as E-cadherin,  $\alpha$ -catenin, and TATA-box binding protein (TBP). Yin *et al.* [31] showed the C-terminal domain is required for the interaction of JUP with Src. Thus, it is most likely the overexpressed C-terminal domain of JUP competes with endogenous JUP for binding to HIF2 $\alpha$  and other cofactors and perturbs the inhibitory effect of JUP.

In addition to interacting with HIF2 $\alpha$ , in the present study, JUP was found to associate with VHL and HDAC1/2 and to decrease the stability and transactivity of HIF2 $\alpha$ . A previous study showed JUP interacts with CUL2 by large-scale immunoprecipitation experiments [43], but the molecular mechanism of this interaction has not been studied. Given JUP facilitates the pVHL-HIF2 $\alpha$  interaction, JUP is likely to directly recruit the pVHL E3 ligase complex to ubiquitinate HIF2 $\alpha$ . The hydroxylation of the oxygen-dependent degradation domain of HIF2 $\alpha$  in normoxic conditions is a prerequisite for VHL binding [44]. However, we found that JUP associated with the PAS/PAC and IH domains of HIF2 $\alpha$ , indicating JUP may be sufficient to promote HIF2 $\alpha$  ubiquitination under both normoxic and hypoxic conditions. HIF $\alpha$  activity is regulated by

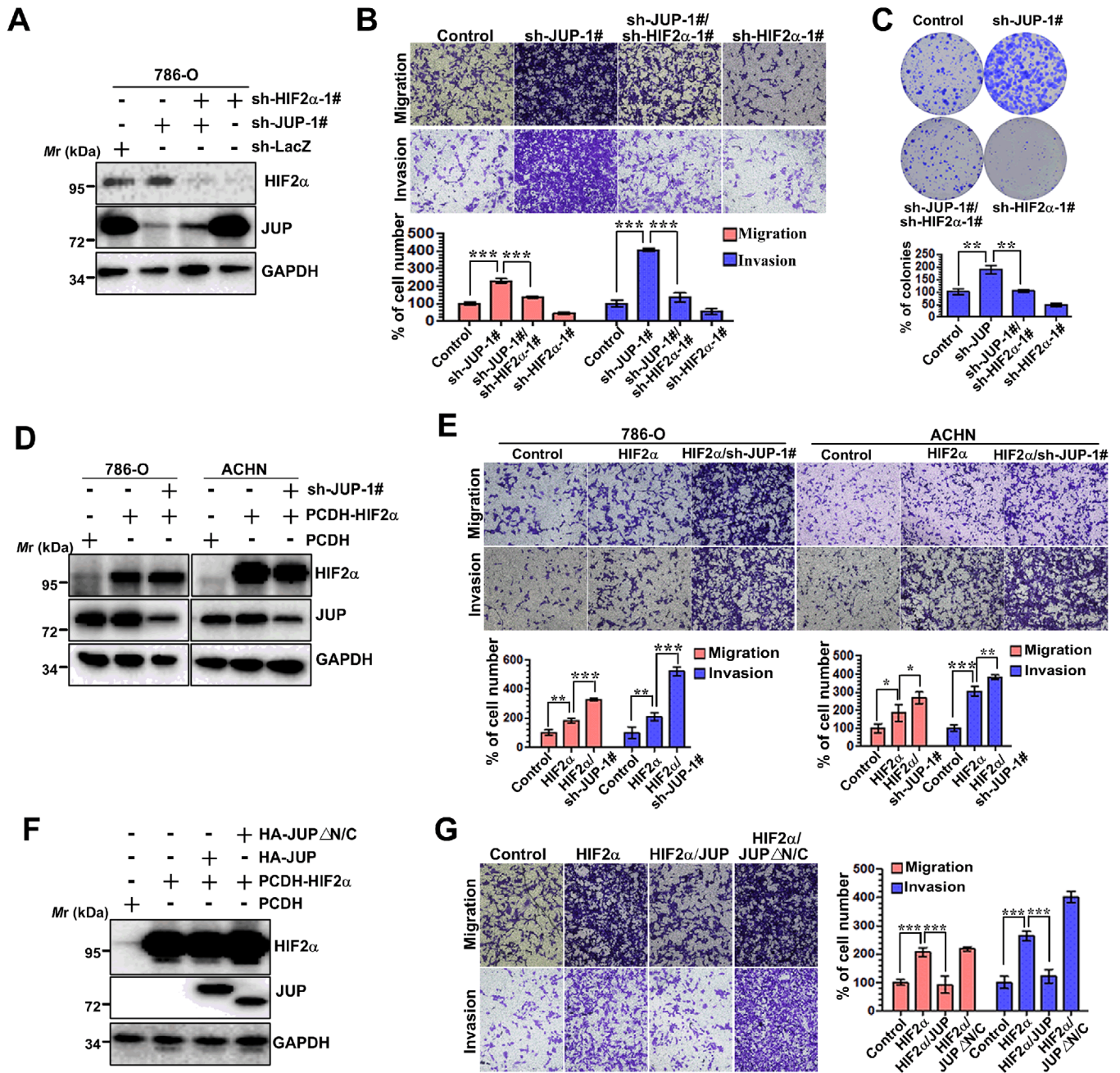


**FIGURE 7** JUP suppresses RCC cell migration and invasion in part through HIF2 $\alpha$ . **A**, 786-O cells were infected with different combinations of lentivirus as indicated. At 72 h after infection, Western blotting analysis was performed to determine the protein levels of JUP and HIF2 $\alpha$ . GAPDH is an internal control. **B** and **C**, 786-O cells stably expressing sh-JUP, sh-HIF2 $\alpha$ , or sh-LacZ as in panel **A** were analyzed by transwell assay (**B**) and colony formation assay (**C**). **D**, ACHN and 786-O cells were infected with lentivirus with control PCDH (Control), PCDH-HIF2 $\alpha$ , or/and sh-JUP as indicated. Western blotting analysis was performed to evaluate the expression of JUP and HIF2 $\alpha$ . GAPDH is an internal control. **E**, After infection as in panel **D**, cells were used for transwell assays. The number of migrated and invaded cells from each group was quantified in 4 random images. **F**, 786-O cells were transfected with PCDH-HIF2 $\alpha$  along with HA-JUP or HA-JUP $\Delta$ N/C, as indicated. Western blotting analysis was performed to determine the protein levels of JUP and HIF2 $\alpha$ . GAPDH is an internal control. **G**, After infection as in panel **D**, cells were used for transwell assays. The number of migrated and invaded cells from each group was quantified in 4 random images. \* $P < 0.05$ , \*\* $P < 0.01$ , and \*\*\* $P < 0.001$ . Abbreviations: JUP, junction plakoglobin; RCC, renal cell carcinoma; JUP $\Delta$ N/C, both N- and C-terminus deletion of JUP

interacting with the transcriptional coactivator p300/CBP and co-repressor HDACs [8, 9]. HDAC1/2, the catalytic core of different co-repressor complexes, is associated with histone deacetylation and silenced genes [45]. In addition, HIF1 $\alpha$ -p300 interaction can be disrupted by HDAC1 [46]. In this context, we found JUP interacted with HDAC1/2 and promoted HDAC1-HIF2 $\alpha$  interaction but was unable to bind p300 (data not shown). Zhao *et al.* [47] found JUP can interact with CBP in imatinib-resistant chronic myeloid leukemia cells. However, it remains unknown if JUP is involved in the HIF2 $\alpha$  switch between association with p300/CBP and HDAC1/2. Various studies have indicated HIF $\alpha$  itself can also be acetylated by p300/CBP and deacetylated by HDACs. For example, Geng *et al.* [46] demonstrated HIF1 $\alpha$  can be acetylated by p300 at Lys-709, which increases its protein stability. They also showed HIF1 $\alpha$  can be deacetylated at Lys-709 by HDAC1. Acetylation also occurs on specific lysine residues of HIF2 $\alpha$  [6, 7]. A critical question is whether HIF2 $\alpha$  acetylation is regulated by the binding of JUP and HDAC1/2. Identification of the components of the JUP complex associated with each functional subset would provide valuable insight into the regulation of HIF2 $\alpha$  signaling.

To date, many studies have investigated the function of JUP in tumorigenesis. Unlike  $\beta$ -catenin, which has well documented oncogenic activities, JUP typically acts as a tumor/metastasis suppressor [29–35]. Loss of total JUP gene expression is frequently observed in primary non-small cell lung cancer [29] and breast cancer [48]. However, some evidence has shown JUP is overexpressed in AML and promotes  $\beta$ -catenin signaling [49], suggesting JUP can also act as an oncogene in a cell-specific context. Most importantly, we analyzed the data from a TCGA ccRCC cohort and found the downregulation of JUP was associated with tumor grade and stage, distant metastasis, and poorer patient survival. Thus, JUP may act as a tumor suppressor in ccRCC development and serve as a potential prognostic marker for ccRCC patients.

Although  $\beta$ -catenin and HIF1 $\alpha$  were not the major subjects of this research, the effects of JUP on  $\beta$ -catenin and HIF1 $\alpha$  activity cannot be ignored. In addition, whether JUP competes with  $\beta$ -catenin for HIF2 $\alpha$  binding is still unknown. The interplay between JUP and ccRCC remains complex, so additional experiments are needed in the future.

## 5 | CONCLUSIONS

In summary, we propose a mechanism by which the tumor suppressor JUP interacts with the HIF2 $\alpha$  transcription factor in ccRCC cells. JUP downregulation is likely to

trigger the aberrant upregulation of HIF2 $\alpha$  stability and transactivity, which further exerts effects on tumorigenesis in ccRCC. These results have important implications in both the diagnosis and treatment of RCC.

## ACKNOWLEDGMENTS

We thank all the patients for their contribution in this study. We thank our group members for all the assistance they provided for this study.

## ETHICS APPROVAL AND CONSENT TO PARTICIPATE

The study was approved by the Institutional Review Board of Huazhong University of Science and Technology, Tongji Medical College, Tongji Hospital. All human tumor tissues were obtained with written informed consent from patients prior to participation in the study.

## CONSENT FOR PUBLICATION

Not applicable.

## AVAILABILITY OF DATA AND MATERIALS

The datasets used and analyzed during the current study are available from the corresponding author on reasonable request.

## DISCLOSURE OF POTENTIAL CONFLICTS OF INTEREST

No potential conflicts of interest were disclosed.

## FUNDING

This work was supported by National Natural Science Foundation of China (grant number 81772721, 81874089, 81602236, 81702522), Natural Science Foundation of Jiangxi Province of China (20202BABL216060), and National Major Scientific and Technological Special Project for “Significant New Drugs Development” (2017ZX09304022). The funders had no role in study design, data collection and analysis, decision to publish, or preparation of the manuscript.

## AUTHORS' CONTRIBUTIONS

HX and KC designed and supervised the project. KC, JZ and YS performed most experiments and data analyses, and helped writing the manuscript. WOY, GY, HZ, WMY, WX, and JHH assisted in performing animal experiments. YJZ and KFX conducted bioinformatic analysis. JCX, LW, ZQC and ZQY proofread this manuscript.

## ORCID

Jin Zeng  <https://orcid.org/0000-0001-9962-8460>

## REFERENCES

- Rodrigues P, Patel SA, Harewood L, Olan I, Vojtasova E, Syafruddin SE, et al. NF- $\kappa$ B-dependent lymphoid enhancer cooption promotes renal carcinoma metastasis. *Cancer Discov*. 2018;8(7):850–65.
- Capitanio U, Montorsi F. Renal cancer. *Lancet*. 2016;387(10021):894–906.
- Maxwell PH, Wiesener MS, Chang G-W, Clifford SC, Vaux EC, Cockman ME, et al. The tumour suppressor protein VHL targets hypoxia-inducible factors for oxygen-dependent proteolysis. *Nature*. 1999;399(6733):271–5.
- Zou JX, Chen K. Roles and molecular mechanisms of hypoxia-inducible factors in renal cell carcinoma. *Yi Chuan*. 2018;40(5):341–56.
- Schodel J, Grampp S, Maher ER, Moch H, Ratcliffe PJ, Russo P, et al. Hypoxia, hypoxia-inducible transcription factors, and renal cancer. *Eur Urol*. 2016;69(4):646–57.
- Dioum EM, Chen R, Alexander MS, Zhang Q, Hogg RT, Gerard RD, et al. Regulation of hypoxia-inducible factor 2 $\alpha$  signaling by the stress-responsive deacetylase sirtuin 1. *Science*. 2009;324(5932):1289–93.
- Chen R, Xu M, Hogg RT, Li J, Little B, Gerard RD, et al. The acetylase/deacetylase couple CREB-binding protein/Sirtuin 1 controls hypoxia-inducible factor 2 signaling. *J Biol Chem*. 2012;287(36):30800–11.
- Arany Z, Huang LE, Eckner R, Bhattacharya S, Jiang C, Goldberg MA, et al. An essential role for p300/CBP in the cellular response to hypoxia. *Proc Natl Acad Sci*. 1996;93(23):12969–73.
- Perez-Perri JI, Acevedo JM, Wappner P. Epigenetics: new questions on the response to hypoxia. *Int J Mol Sci*. 2011;12(7):4705–21.
- Chen Y, Zhang B, Bao L, Jin L, Yang M, Peng Y, et al. ZMYND8 acetylation mediates HIF-dependent breast cancer progression and metastasis. *J Clin Invest*. 2018;128(5):1937–55.
- D'Ignazio L, Bandarra D, Rocha S. NF- $\kappa$ B and HIF crosstalk in immune responses. *FEBS J*. 2016;283(3):413–24.
- Bracken CP, Whitelaw ML, Peet DJ. Activity of hypoxia-inducible factor 2 $\alpha$  is regulated by association with the NF- $\kappa$ B essential modulator. *J Biol Chem*. 2005;280(14):14240–51.
- Mutvei AP, Landor SKJ, Fox R, Braune E-B, Tsoi YL, Phoon YP, et al. Notch signaling promotes a HIF2 $\alpha$ -driven hypoxic response in multiple tumor cell types. *Oncogene*. 2018;37(46):6083–95.
- Johnson EA. HIF Takes It Up a Notch. *Sci Signal*. 2011;4(181):pe33.
- Choi H, Chun Y-S, Kim T-Y, Park J-W. HIF-2 $\alpha$  enhances  $\beta$ -catenin/TCF-driven transcription by interacting with  $\beta$ -catenin. *Cancer Res*. 2010;70(24):10101–11.
- Zhang Q, Lou Y, Zhang J, Fu Q, Wei T, Sun X, et al. Hypoxia-inducible factor-2 $\alpha$  promotes tumor progression and has crosstalk with Wnt/ $\beta$ -catenin signaling in pancreatic cancer. *Mol Cancer*. 2017;16(1):119.
- Chen W, Hill H, Christie A, Kim MS, Holloman E, Pavia-Jimenez A, et al. Targeting renal cell carcinoma with a HIF-2 antagonist. *Nature*. 2016;539(7627):112–7.
- Cho H, Du X, Rizzi JP, Liberzon E, Chakraborty AA, Gao W, et al. On-target efficacy of a HIF-2 $\alpha$  antagonist in preclinical kidney cancer models. *Nature*. 2016;539(7627):107–11.
- Wallace EM, Rizzi JP, Han G, Wehn PM, Cao Z, Du X, et al. A small-molecule antagonist of HIF2 $\alpha$  is efficacious in preclinical models of renal cell carcinoma. *Cancer Res*. 2016;76(18):5491–500.
- Courtney KD, Infante JR, Lam ET, Figlin RA, Rini BI, Brugarolas J, et al. Phase I dose-escalation trial of PT2385, a first-in-class hypoxia-inducible factor-2 $\alpha$  antagonist in patients with previously treated advanced clear cell renal cell carcinoma. *J Clin Oncol*. 2017;Jco2017742627.
- Chen K, Yu G, Gumireddy K, Li A, Yao W, Gao L, et al. ZBRK1, a novel tumor suppressor, activates VHL gene transcription through formation of a complex with VHL and p300 in renal cancer. *Oncotarget*. 2015;6(9):6959–76.
- Chen K, Zeng J, Xiao H, Huang C, Hu J, Yao W, et al. Regulation of glucose metabolism by p62/SQSTM1 through HIF1 $\alpha$ . *J Cell Sci*. 2016;129(4):817–30.
- Chen K, Huang C, Yuan J, Cheng H, Zhou R. Long-term artificial selection reveals a role of TCTP in autophagy in mammalian cells. *Mol Biol Evol*. 2014.
- Liu J, Lichtenberg T, Hoadley KA, Poisson LM, Lazar AJ, Cherniack AD, et al. An integrated TCGA pan-cancer clinical data resource to drive high-quality survival outcome analytics. *Cell*. 2018;173(2):400–16.e11.
- Bhandari V, Hoey C, Liu LY, Lalonde E, Ray J, Livingstone J, et al. Molecular landmarks of tumor hypoxia across cancer types. *Nature Genetics*. 2019;51(2):308–18.
- Ragnum HB, Vlatkovic L, Lie AK, Axcrone K, Julin CH, Friksstad KM, et al. The tumour hypoxia marker pimonidazole reflects a transcriptional programme associated with aggressive prostate cancer. *Br J Cancer*. 2015;112(2):382–90.
- Robinson MD, McCarthy DJ, Smyth GK. edgeR: a Bioconductor package for differential expression analysis of digital gene expression data. *Bioinformatics*. 2010;26(1):139–40.
- Huang LE. Carrot and stick: HIF- $\alpha$  engages c-Myc in hypoxic adaptation. *Cell Death Differ*. 2008;15:672.
- Winn RA, Bremnes RM, Bemis L, Franklin WA, Miller YE, Cool C, et al. gamma-Catenin expression is reduced or absent in a subset of human lung cancers and re-expression inhibits transformed cell growth. *Oncogene*. 2002;21(49):7497–506.
- Rieger-Christ KM, Ng L, Hanley RS, Durrani O, Ma H, Yee AS, et al. Restoration of plakoglobin expression in bladder carcinoma cell lines suppresses cell migration and tumorigenic potential. *Br J Cancer*. 2005;92(12):2153–9.
- Yin T, Getsios S, Caldelari R, Kowalczyk AP, Muller EJ, Jones JC, et al. Plakoglobin suppresses keratinocyte motility through both cell-cell adhesion-dependent and -independent mechanisms. *Proc Natl Acad Sci U S A*. 2005;102(15):5420–5.
- Sechler M, Borowicz S, Van Scoyk M, Avsarala S, Zerayesus S, Edwards MG, et al. Novel role for gamma-catenin in the regulation of cancer cell migration via the induction of hepatocyte growth factor activator inhibitor type 1 (HAI-1). *J Biol Chem*. 2015;290(25):15610–20.
- Charpentier E, Lavker RM, Acquista E, Cowin P. Plakoglobin suppresses epithelial proliferation and hair growth in vivo. *J Cell Biol*. 2000;149(2):503–20.
- Aktary Z, Chapman K, Lam L, Lo A, Ji C, Graham K, et al. Plakoglobin interacts with and increases the protein levels of metastasis suppressor Nm23-H2 and regulates the expression of Nm23-H1. *Oncogene*. 2010;29(14):2118–29.



35. Lam L, Aktary Z, Bishay M, Werkman C, Kuo CY, Heacock M, et al. Regulation of subcellular distribution and oncogenic potential of nucleophosmin by plakoglobin. *Oncogenesis*. 2012;1:e4.
36. Yao X, Tan J, Lim KJ, Koh J, Ooi WF, Li Z, et al. VHL deficiency drives enhancer activation of oncogenes in clear cell renal cell carcinoma. *Cancer Discov*. 2017;7(11):1284–305.
37. Aktary Z, Alaei M, Pasdar M. Beyond cell-cell adhesion: plakoglobin and the regulation of tumorigenesis and metastasis. *Oncotarget*. 2017;8(19):32270–91.
38. Aktary Z, Pasdar M. Plakoglobin: role in tumorigenesis and metastasis. *Int J Cell Biol*. 2012;2012:189521.
39. Kaidi A, Williams AC, Paraskeva C. Interaction between  $\beta$ -catenin and HIF-1 promotes cellular adaptation to hypoxia. *Nat Cell Biol*. 2007;9:210.
40. Zhang Q, Bai X, Chen W, Ma T, Hu Q, Liang C, et al. Wnt/ $\beta$ -catenin signaling enhances hypoxia-induced epithelial-mesenchymal transition in hepatocellular carcinoma via crosstalk with hif-1 $\alpha$  signaling. *Carcinogenesis*. 2013;34(5):962–73.
41. Criscimanna A, Duan L-J, Rhodes JA, Fendrich V, Wickline E, Hartman DJ, et al. PanIN-specific regulation of Wnt signaling by HIF2 $\alpha$  during early pancreatic tumorigenesis. *Cancer Res*. 2013;73(15):4781–90.
42. Solanas G, Miravet S, Casagolda D, Castano J, Raurell I, Corriero A, et al.  $\beta$ -catenin and plakoglobin N- and C-tails determine ligand specificity. *J Biol Chem*. 2004;279(48):49849–56.
43. Kristensen AR, Gsponer J, Foster LJ. A high-throughput approach for measuring temporal changes in the interactome. *Nat Methods*. 2012;9(9):907–9.
44. Maxwell PH, Wiesener MS, Chang GW, Clifford SC, Vaux EC, Cockman ME, et al. The tumour suppressor protein VHL targets hypoxia-inducible factors for oxygen-dependent proteolysis. *Nature*. 1999;399(6733):271–5.
45. Wong MM, Guo C, Zhang J. Nuclear receptor corepressor complexes in cancer: mechanism, function and regulation. *Am J Clin Exp Urol*. 2014;2(3):169–87.
46. Geng H, Liu Q, Xue C, David LL, Beer TM, Thomas GV, et al. HIF1 $\alpha$  protein stability is increased by acetylation at lysine 709. *J Biol Chem*. 2012;287(42):35496–505.
47. Zhao Y, Masiello D, McMillian M, Nguyen C, Wu Y, Melendez E, et al. CBP/catenin antagonist safely eliminates drug-resistant leukemia-initiating cells. *Oncogene*. 2016;35(28):3705–17.
48. Paredes J, Correia AL, Ribeiro AS, Milanezi F, Cameselle-Teijeiro J, Schmitt FC. Breast carcinomas that co-express E- and P-cadherin are associated with p120-catenin cytoplasmic localisation and poor patient survival. *J Clin Pathol*. 2008;61(7):856–62.
49. Morgan RG, Pearn L, Liddiard K, Pumford SL, Burnett AK, Tonks A, et al.  $\gamma$ -Catenin is overexpressed in acute myeloid leukemia and promotes the stabilization and nuclear localization of  $\beta$ -catenin. *Leukemia*. 2013;27(2):336–43.

## SUPPORTING INFORMATION

Additional supporting information may be found online in the Supporting Information section at the end of the article.

**How to cite this article:** Chen K, Zeng J, Sun Y, et al. Junction plakoglobin regulates and destabilizes HIF2 $\alpha$  to inhibit tumorigenesis of renal cell carcinoma. *Cancer Commun*. 2021;41:316–332. <https://doi.org/10.1002/cac2.12142>